Proc. 3rd Int. Symp. on Turbulence and Shear Flow Phenomena
Sendai, Japan, June 25-27, 2003

EVALUATION OF GA-BASED FEEDBACK CONTROL SYSTEM FOR DRAG REDUCTION IN WALL TURBULENCE

Takashi Yoshino, Yuji Suzuki, and Nobuhide Kasagi
Department of Mechanical Engineering,
The University of Tokyo
Hongo, Bunkyo-ku, Tokyo 113-8656, Japan
yoshino@thtlab.t.u-tokyo.ac.jp, ysuzuki@thtlab.t.u-tokyo.ac.jp, kasagi@thtlab.t.u-tokyo.ac.jp

ABSTRACT

A prototype feedback control system for wall turbulence is developed and evaluated in a turbulent channel flow. Arrayed micro hot-film sensors with a spanwise spacing of 1 mm are employed for the measurement of streamwise wall shear stress fluctuations, while arrayed magnetic actuators with 3 mm in spanwise width are used to introduce control input through wall deformation. The frequency response of the sensors and actuators is found to be reasonably high for the flow conditions presently considered. A digital signal processor with a time delay of 1.6 ms is employed to drive output voltage for the actuators. Feedback control experiments are made in a turbulent air channel flow with the aid of a genetic algorithm-based optimal control scheme. It is found that the root-mean-square value of the wall shear stress fluctuations is decreased by up to 9 % among 100 trials in 10 generations. Attempts to develop the micro sensors having higher response are also discussed.

INTRODUCTION

In the last decade, feedback control of wall turbulence attracts much attention because of its potential of high control performance with a small energy input (e.g., Moin & Bewley, 1994; Gad-el-Hak, 1996; Kasagi, 1998). In such a control system, the near-wall coherent structures, which are responsible for the turbulent transport mechanisms, should be detected by sensors mounted on the wall, and selectively manipulated by the motion of actuators. Since the coherent structures have generally very small spatio-temporal scales, it is difficult to perform experiments. However, recent development of microelectromechanical systems (MEMS) technology has made it possible to fabricate flow sensors and mechanical actuators of submillimeter scale (Ho and Tai, 1998). Tsao et al. (1997) and Rathnasingham and Breuer (1997) separately built early prototypes of the feedback control system. However, the number of sensors/actuators is limited in their experiment, and direct evaluation of the control was not made.

Recently, Endo et al. (2000) carried out direct numerical simulations (DNS) of a turbulent channel flow, in which arrayed wall shear stress sensors and wall-deformation actuators of finite spatial dimensions are assumed. They devised a practical control algorithm based on physical arguments on the near-wall coherent structures, and obtained 12 % drag reduction by attenuating the near-wall streamwise vortices. Morimoto et al. (2002) employed genetic algorithms to develop optimal control scheme based on the streamwise wall shear stress fluctuations. They obtained drag reduction of 12 % by using local wall blowing/suction. These findings encourage us to develop a feedback control system for wall turbulence.

The objectives of the present study are to develop a prototype of feedback control system with arrayed micro hot-film shear stress sensors and wall-deformation actuators, and to evaluate its performance in a turbulent air channel flow.

FEEDBACK CONTROL SYSTEM FOR TURBULENT CHANNEL FLOW

Figure 1 shows a schematic diagram of feedback control system for wall turbulence. Several rows of arrayed micro sensors aligned in the spanwise direction are mounted flush on the wall, and arrays of actuators are placed in between. These devices are designed in such a way that the near-wall streamwise vortices are detected based on wall valuables and manipulated by the motion of actuators. In the present study, hot-film sensors are employed for the measurement of the streamwise wall shear stress, while magnetic actuators are used to introduce control input into the flow field by wall deformation.

Requirements for the spatio-temporal scales of actuators are estimated from our previous DNS. Figure 2 shows contours of the two-point correlation coefficient of blowing/suction control input on the wall (Morimoto et al., 2002). The region of high correlation coefficient is confined in the area of $-20<\Delta z^+<20$ and $-100<\Delta x^+<100$. Therefore, the spanwise and streamwise lengths of the actuator should be smaller than 40 and 200 viscous units, respectively. Those dimensions are in accordance with the DNS result of Endo et al. (2000), where the typical length scale of wall deformation is elongated in the streamwise direction. Morimoto et al. (2002) shown that time spectra of the wall shear stress fluctuations and the control input exhibits a sharp drop at $f^+=0.1$ (not shown here). Therefore, the requirement for the time scale of sensors and actuators is $f^+=0.1$, which corresponds to about 300 Hz at $Re_\tau=300$.

Figure 3 shows a prototype control system, which consists of four rows of 48 hot-film sensor arrays with a spanwise spacing of 1 mm and three rows of 16 wall-deformation electromagnetic actuators with a spanwise spacing of 3.2 mm. The

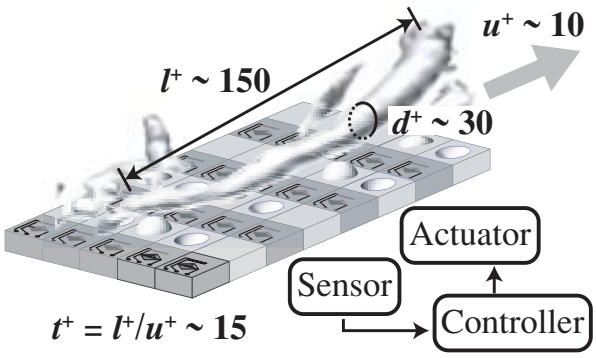

Figure 1 Schematic diagram of active feedback control system for wall turbulence.

spanwise lengths of the sensors and actuators are about 25 and 35 wall units at Re_τ=300, respectively, which are in accordance with the aforementioned requirements. The streamwise distance of each row of the arrayed sensors is 20.9 mm, which corresponds to 252 wall units. In the present study, 23 sensors in the first three rows are selected for the feedback sensor in such a way that their spanwise spacing is 3.2 mm. On the other hand, 16 actuators are employed for the control experiment. Five sensors (evaluators) in the last row are used to evaluate cost function.

A digital signal processor (DSP) board (SMT-326, Sundance DSP Inc.) with 32 analog inputs/output channels is used as the controller of the present system. The output voltage of the constant temperature circuits for the hot-film sensors is firstly digitized with the 16 bit AD converters. The control signals for the actuators are then computed with the DSP (C44, 60MFLOPS) and converted back to analog signals using the 16 bit DA converters. The present DSP system has an inherent time delay of 1.6 ms due to the internal data transfer and processing.

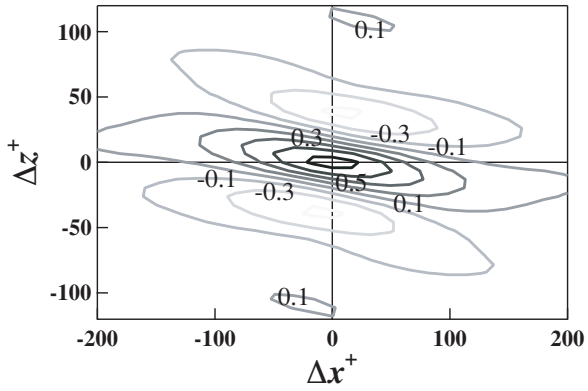

Figure 2 Contours of two-point correlation of the blowing/suction control input in DNS of GA-based feedback control of turbulent channel flow (Suzuki et al., 2001).

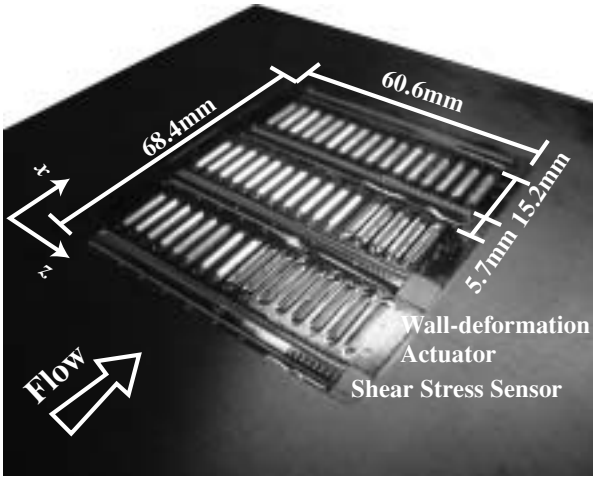

Figure 3 Prototype of the feedback control system with arrayed sensors and actuators.

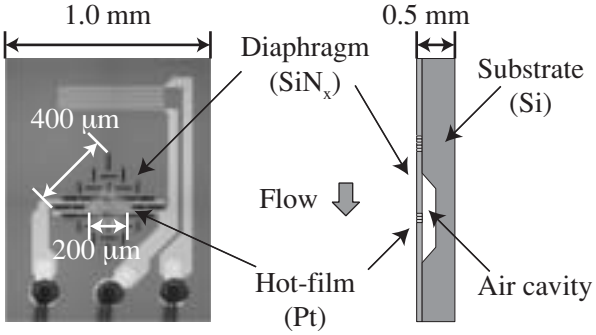

Figure 4 Magnified view of micro hot-film shear stress sensor.

A turbulent air channel flow facility is employed for the present experiment. The cross section is 50×500 mm^2, and the test section is located 4 m downstream from the inlet, where the flow is fully developed. The control system is placed at the bottom wall of the test section. The bulk mean velocity U_m is varied from 2.5 to 9.3 m/s, which corresponds to the Reynolds number Re_τ based on the wall friction velocity u_τ and the channel half-width of 250 to 800. When Re_τ=300 (U_m=3.0 m/s), one viscous length and time units correspond to 0.08 mm and 0.5 ms, respectively. At this flow condition, the mean diameter of the near-wall streamwise vortices is estimated to be 2.4 mm, while its characteristic time scale is 7.5 ms. The deformation of the actuator is measured with a laser displacement meter (Keyence Inc., LC-2450) through a glass window mounted on the top wall of the channel.

MICRO WALL SHEAR STRESS SENSOR

Figure 4 shows a schematic of the micro shear stress sensor used in the present study (Yoshino et al., 2001). A platinum thin-film heater is deposited on a SiN_x diaphragm of 1 μm in thickness. In order to keep sufficiently large electric resistance of the heater, a thin line of platinum is patterned zigzag in an area of 200×23 μm^2. An air cavity of 200 μm in depth is formed underneath the diaphragm (400×400 μm^2) for reducing thermal loss to the substrate. Another platinum resis-

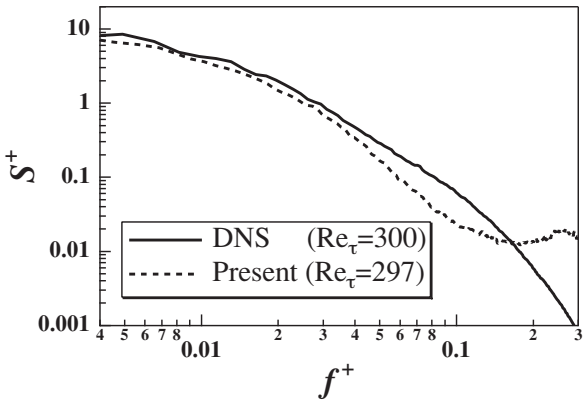

Figure 5 Power spectra of the streamwise shear stress fluctuations.

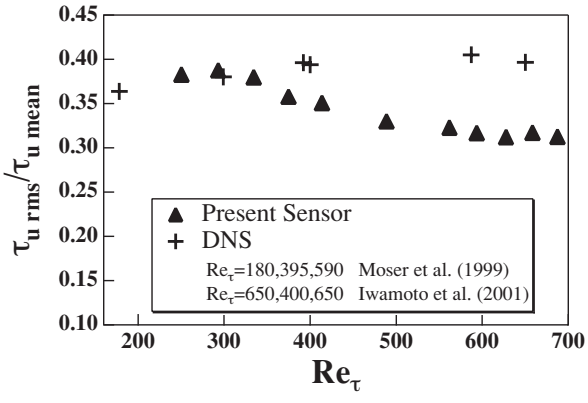

Figure 6 RMS values of the wall shear stress fluctuations.

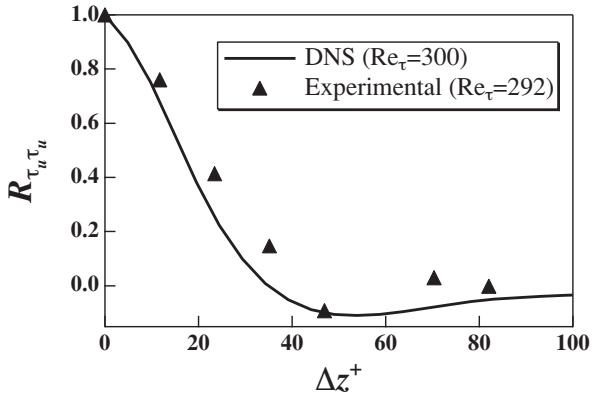

Figure 7 Spanwise two-point correlation of the streamwise shear stress fluctuations.

tor is made on the substrate and used for temperature compensation.

Figure 5 shows the power spectra of the streamwise shear stress in comparison with the DNS study of Iwamoto et al. (2002). The frequency response is surprisingly low and is flat up to only 40 Hz (f^+=0.02) at Re$_\tau$=300. Figure 6 shows the root-mean-square value of the streamwise wall shear stress $\tau_{w\,rms}$ normalized by its mean value $\tau_{w\,mean}$. It is found in previous DNS studies (Moser et al., 1999; Iwamoto et al., 2002) that $\tau_{w\,rms}/\tau_{w\,mean}$ is weakly dependent on the Reynolds number and equal to about 0.36-0.4. The present measurement data are decreased with increasing the Reynolds number due to the imperfect response of the sensor. However, the error in $\tau_{w\,rms}/\tau_{w\,mean}$ is relatively small at Re$_\tau$=300. The spanwise two-point correlation of τ_w measured with the arrayed sensors is shown in Fig. 7. The correlation exhibits a negative peak at Δz^+~50, and is in good accordance with the DNS data (Iwamoto et al. 2002). Therefore, it is conjectured that the near-wall coherent structures, which are the target of the feedback control, can be well captured with the present wall shear stress sensors.

WALL-DEFORMATION MAGNETIC ACTUATOR

Figure 8 shows a schematic of the wall-deformation magnetic actuator elongated in the streamwise direction. A silicone rubber sheet of 0.1 mm in thickness is used as an elastic membrane, and a rare-earth rectangular permanent magnet of 10×1 mm^2 with 1 mm in thickness is glued on its backside. A miniature copper coil (250 turns), of which outer width, length and height are respectively 2.4 mm, 14 mm and 4 mm, is placed underneath the magnet with a 0.4 mm gap. Figure 9 shows a static response of the actuator. The wall displacement is a nonlinear function of the voltage applied, and about 200 μm displacement is obtained at the center of the actuator with a 12 V voltage input. The dynamic response of the actuator for sinusoidal driving voltage is shown in Fig. 10. The resonant frequency is 600 Hz for 12 Vp-p signals with a maximum amplitude of 0.25 mm. Therefore, the response of the actuator satisfies the requirement at Re$_\tau$=300.

OPTIMAL FEEDBACK CONTROL BASED ON GENETIC ALGORITHM

An optimal control scheme based on genetic algorithm (GA) is employed in the present experiment (Morimoto et al., 2002). Driving voltage of each actuator E_A is determined with a linear combination of the streamwise wall shear stress fluctuations $\tau_w'_i$, i.e.,

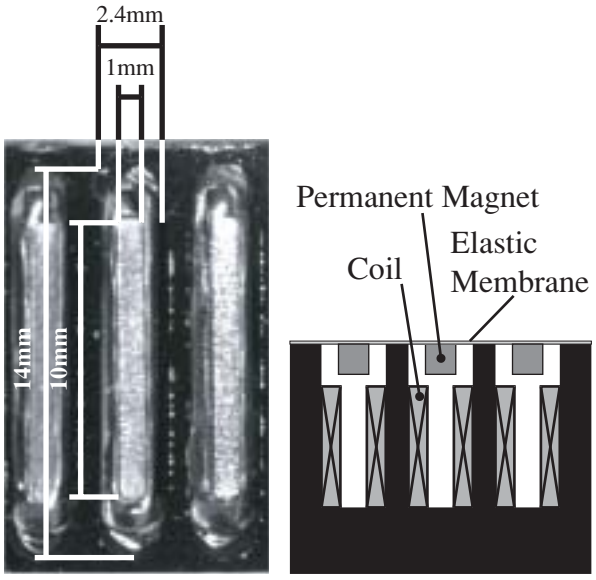

Figure 8 Magnified view of wall-deformation magnetic actuator.

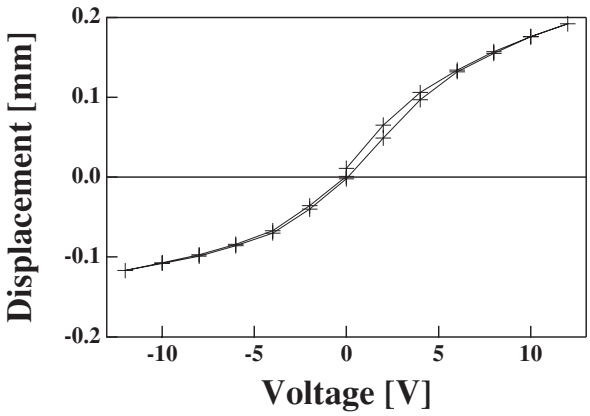

Figure 9 Static response of wall-deformation magnetic actuator.

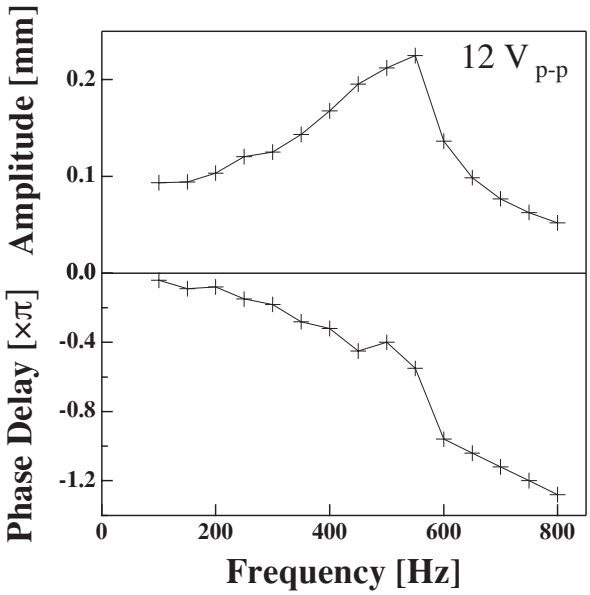

Figure 10 Dynamic response of wall-deformation magnetic actuator.

$$E_A = \sum_{i=1}^{3} C_i \cdot \tau_{w}{}'_{i}, \quad (1)$$

where $\tau_w{}'_i$ is measured with sensors located upstream of the actuator aligned in the spanwise direction; C_2 is the weight of τ_w' measured just upstream the actuator, and C_1 and C_3 are the weights of τ_w' at a spanwise distance of $\Delta z^+ \sim \pm 40$ from the actuator. The control variable C_i is optimized in such a way that a cost function based on the wall shear stress fluctuations $\tau_w{}'_j$ measured by the evaluators given by

$$J = \sum_{j=1}^{5} \int_{t}^{t+\Delta T} \tau_{w}{}'^{2}_{j}\, dt, \quad (2)$$

is minimized. A single set of C_i is employed to drive all the actuators.

A binary-coded string with 5 bits, which corresponds to a single gene, is employed to represent each C_i, and each individual consists of three genes. Firstly, N individuals are generated with random numbers. Then, feedback control experiments using each individual, i.e., a different set of C_i is independently carried out, and the cost function is calculated online. Individuals having smaller cost is statistically selected as parents, and two offspring are made through so-called crossover operation between them. In total, N children are created by applying the crossover operation $N/2$ times. Finally, mutation at a given rate of 0.2 is applied to the individuals. New generations are successively produced by repeating this procedure. Optimal solution is obtained when the evolution is found to be in convergence. Population size N and the number of generation are chosen as 10 and 10, respectively, so that 100 trials with different sets of the control variables are made in total. The integration time ΔT is chosen as 40 s (ΔT^+=8000).

Figure 11(a) shows the time traces of E_A and the displacement of the magnetic actuator. The frequency of the control loop is about 6 kHz. The cross correlation of these signals exhibits a marked peak at 2.2 ms (Fig. 11b), which corresponds to a time delay of the present control loop. Thus, the time delay is slightly larger than the mean traveling time of the streamwise vortices between neighboring sensors and actuators, which is estimated to be 1.9 ms. Since the major part of the time delay is caused by the DSP itself, a faster controller is required for better response of the control system.

Figure 12 shows the root-mean-square value of τ_w' versus the generation of the GA-based control scheme. Maximum reduction of 9 % is obtained at Generation 4. Figure 13 shows distribution of C_i giving $\tau_{w\,rms}/\tau_{w\,rms\,0}<1$ after Generation 4. Except C_i for the 6th generation, they exhibit similar tendency; C_2 is negative and C_1 and C_3 are positive. Since C_2 is the weight of τ_w' at $\Delta z^+=0$, the actuators should move upward when the low-speed streak is located at the center of actuator. The present result for the optimal distribution of C_i is different from the DNS results of Morimoto et al. (2002), where antisymmetric distribution of C_i is effective in reducing skin friction. This is probably because the number of generation in the present control experiment is not sufficient to achieve the convergence.

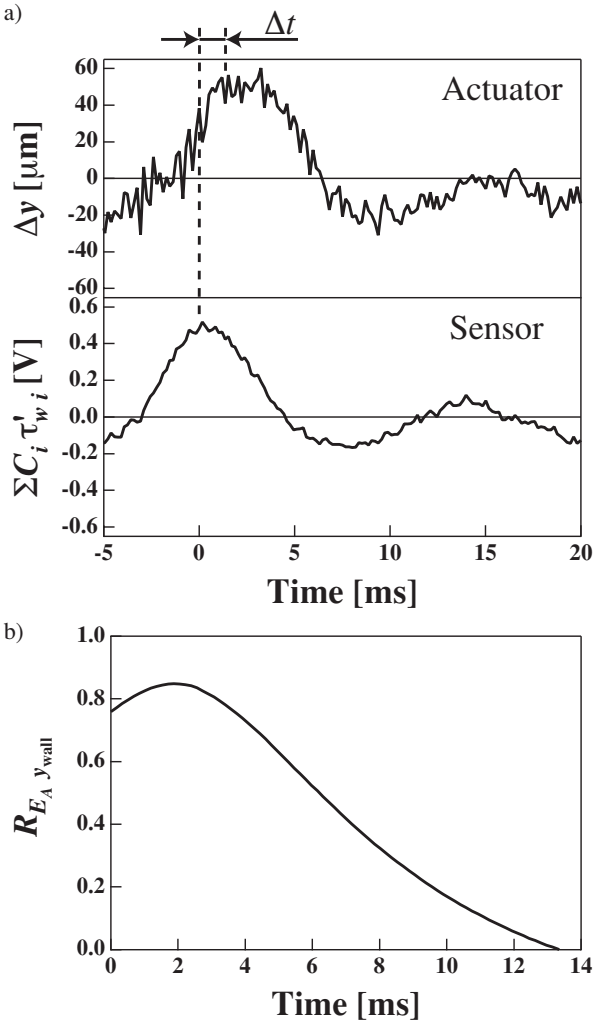

Figure 11 Response of the GA-based feedback control System. a) Time traces of actuator displacement Δy and the actuator driving voltage E_A, b) Cross correlation of E_A and Δy.

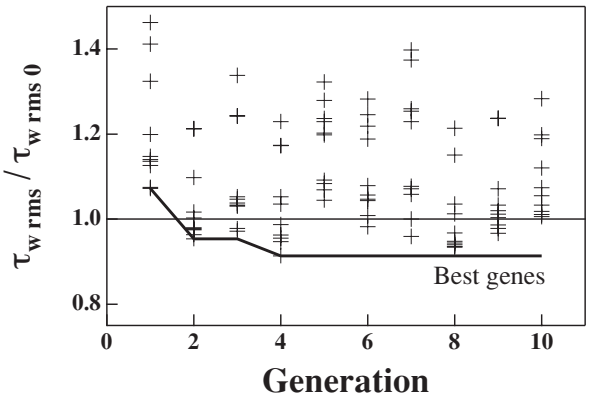

Figure 12 RMS value of the wall shear stress fluctuations versus generation of the GA-based control algorithm.

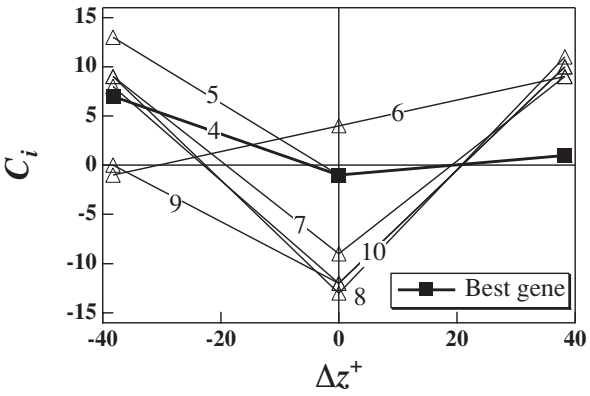

Figure 13 Distribution of the best control parameters C_i at each generation.

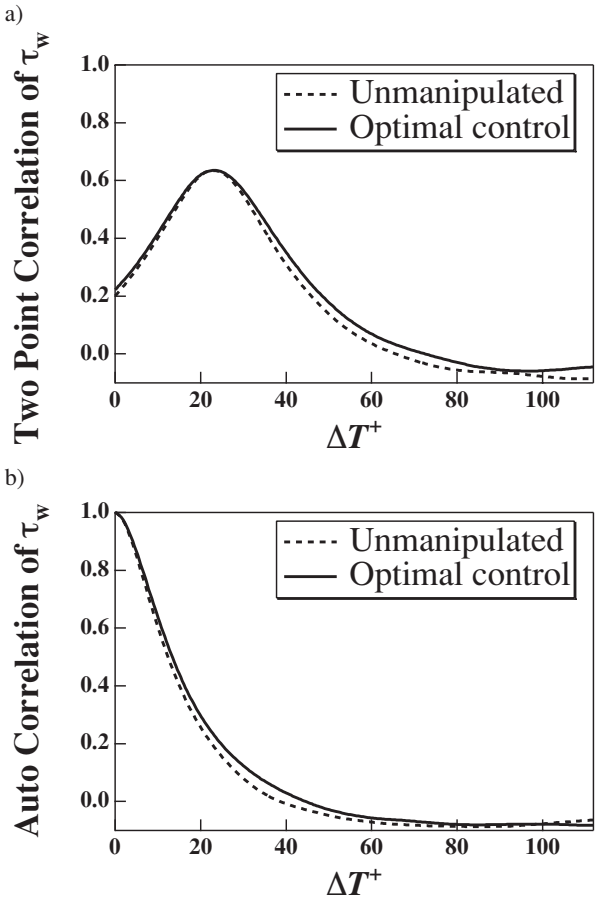

Figure 14 Correlation coefficients of the streamwise shear stress fluctuations at the evaluation sensor. a) Streamwise two-point correlation with the fluctuations at Δx^+=252 upstream of the evaluation sensor, b) Auto correlation coefficient.

Figure 14a shows the streamwise two-point correlation of the streamwise shear stress fluctuations for Δx^+=252, measured with sensors in the 3rd row and at the evaluator sensor. A positive peak corresponds to the traveling time of the near-wall coherent structures between the two sensors. Two-point correlation under the present optimal control is increased at ΔT^+>22. Auto correlation coefficient of the streamwise shear stress fluctuations at the evaluator is shown in Fig. 14b. Again, the auto correlation is increased for large ΔT^+. It is conjectured that the streaky structures becomes more stable and/or less meanders with the present control.

IMPROVEMENT OF MICRO HOT-FILM SHEAR STRESSSENSOR

Our first generation sensor has two drawbacks. Firstly, the frequency response is insufficient as shown in Fig. 5, and it should be improved for its application to higher Reynolds number flows. Secondarily, the electric contact has to be made on the top surface of the sensor using wire bonding, so that the gold wires protruding from the wall should contribute to the large form drag, even though the profusion height is within the viscous sublayer.

We made a series of numerical simulation of the thermal field around the hot-film sensor (Yoshino et al., 2003) in order to improve its frequency response. Sensor models having thermal insulation slits on the both sides of the hot-film are exam-

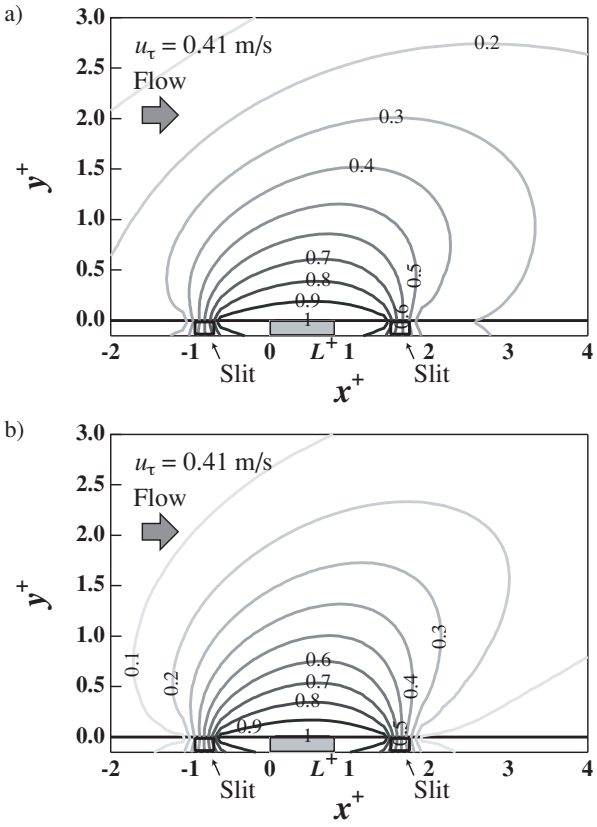

Figure 15 Temperature distribution around the hot-film on the diaphragm having slits on the both sides of the hot-film. a) Sensor model having a diaphragm length of 700 μm, b) Sensor model having a diaphragm length of 200 μm.

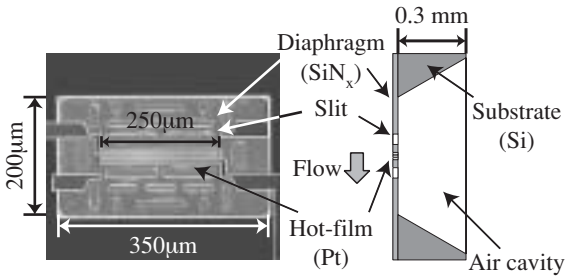

Figure 16 Magnified view of micro hot-film shear stress sensor having improved dynamic response.

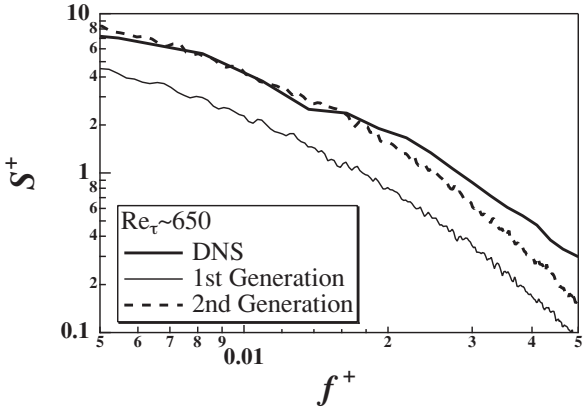

Figure 17 Comparison of power spectrum of the wall shear stress versus the DNS data of turbulent channel flow (Iwamoto et al., 2002).

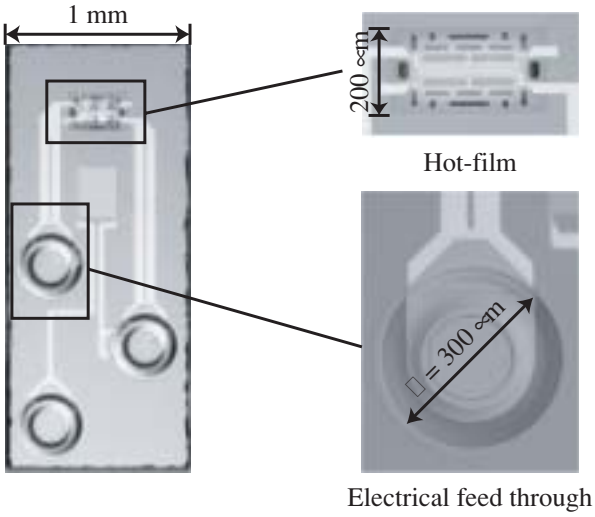

Figure 18 Prototype of wall shear stress sensor having the backside electric contact.

ined, and their frequency response is numerically investigated. It is well known that the heat conduction loss to the substrate deteriorates the sensor response (e.g., Alfredson et al., 1988), but it is not the case. It turns out that the heat conduction in the fluid is responsible for the imperfect frequency response of the sensor. Figure 15 shows temperature distribution around the hot-film. When the diaphragm length W is 700 μm, which is similar to our first generation sensor (W=500 μm), isothermal contours are extended even upstream, and inhibits the hot-film from being exposed to the ambient temperature fluid. On the other hand, when W=200 μm, the slits on the diaphragm work well for the thermal conduction barrier, and the temperature distribution markedly shrinks.

Figure 16 shows our second-generation sensor based on the numerical analysis. The diaphragm length is designed to be 200 μm. As shown in Fig. 17, the frequency response of the 2nd generation sensor is markedly improved over that of our first-generation sensor, and the power spectra is in good agreement with the DNS data of Iwamoto et al. (2002).

Attempt to fabricate sensors having backside electrical contact is also made using a novel MEMS technology for the electrical feed through (Fig. 18). With this fabrication technique, electrical pads are fabricated on the backside of the Silicon substrate, so that no wiring cables are required on the topside. Arrayed sensors having the backside contact with a 1 mm spanwise spacing is now under development, and will be integrated into our next generation control system.

CONCLUSIONS

A prototype of the feedback control system for turbulent channel flow is developed with arrayed micro hot-film sensors and wall-deformation magnetic actuators. Dynamic response of the sensors and actuators are found to be fast enough to capture characteristic time scale of streamwise vortices for the experimental condition employed. A genetic algorithm-based control scheme is successfully implemented on a DSP controller. Control variables are optimized in such a way that the time integral of the wall shear stress fluctuations is minimized. It is found that the root-mean-square value of the wall shear stress fluctuation is decreased by 9% among 100 trials in 10 generations. Sensors having improved frequency response and backside electrical feed through are also developed for the next generation control system.

ACKNOWLEDGMENTS

The authors are grateful to Messrs. S. Kamiunten and N. Zushi in Yamatake Corp. for their corporation in fabrication of the micro shear stress sensors. The authors also thank to Mr. Imakita for his aid in his laboratory work. This work was supported through the Project for Organized Research Combination System by the Ministry of Education, Culture, Sports, Science and Technology of Japan (MEXT).

REFERENCES

Alfredsson, P. H., Johansson, A. V., Haritonidis, J. H., and Eckelmann, H., 1988, "The fluctuating wall-shear stress and the velocity field in the viscous sublayer", *Phys. Fluids*, 31, pp. 1026-1033.

Endo, T., Kasagi, N., and Suzuki, Y., 2000, "Feedback control of wall turbulence with wall deformation," *Int. J. Heat & Fluid Flow*, 21, pp. 568-575.

Gad-el-Hak, M., 1996, "Modern developments in flow control," *Appl. Mech. Rev.*, 49, pp. 365-379.

Ho, C. M., and Tai, Y. C., 1998, "Micro-electro-mechanical-systems (MEMS) and fluid flows," *Annu. Rev. Fluid Mech.*, 30, pp. 579-612.

Iwamoto, K., Suzuki, Y., and Kasagi, N., 2002, "Reynolds number effect on wall turbulence: toward effective feedback control," *Int. J. Heat & Fluid Flow*, 23, pp. 678-689.

Kasagi, N., 1998, "Progress in direct numerical simulation of turbulent transport and its control," *Int. J. Heat & Fluid Flow*, 19, pp. 125-134.

Moin, P., and Bewley, T., 1994, "Feedback control of turbulence," *Appl. Mech. Rev.*, 47, pp. S3-S13.

Morimoto, K., Iwamoto, K., Suzuki, Y., and Kasagi, N., 2002, "Genetic Algorithm-Based Optimization of Feedback Control Scheme for Wall Turbulence," *Proc. 3rd Symp. Smart Control of Turbulence*, Tokyo, pp. 107-113.

Moser, R. D., Kim, J., and Mansour, N. N., 1999, "Direct numerical simulation of turbulent channel flow up to Re_τ=590," *Phys. Fluids*, 11, pp. 943-945.

Rathnasingham, R., and Breuer, K., 1997, "System identification and control of a turbulent boundary layer," *Phys. Fluids*, 9, pp. 1867-1869.

Tsao, T., Jiang, F., Miller, R., Tai, Y.-C., Gupta, B., Goodman, R., Tung, S., and Ho, C.-M., 1997, "An integrated MEMS system for turbulent boundary layer control," *Int. Conf. on Solid-State Sensors and Actuator (Transducers '97)*, Chicago, 2, pp. 315-317.

Yoshino, Y., Suzuki, Y., Kasagi, N., and Kamiunten, S., 2001, "Assessment of the wall shear stress measurement with arrayed micro hot-film sensors in a turbulent channel flow," *2nd Int. Symp. Turbulence and Shear Flow Phenomena*, Stockholm, II, pp. 153-158.

Yoshino, Y., Suzuki, Y., Kasagi, N., and Kamiunten, S., 2003, "Optimum design of micro thermal flow sensor and its evaluation in wall shear stress measurement," *Proc. IEEE Int. Conf. MEMS 2003*, Kyoto, pp. 193-196.